



Wettability Alteration Induced by Surface Roughening During Low Salinity Waterflooding

Taufan Marhaendrajana^{*}, Muhammad Ghifari Ridwan, Maulana Insan Kamil & Pudji Permadi

Petroleum Engineering Department, Faculty of Mining and Petroleum Engineering, Institut Teknologi Bandung, Jalan Ganesa No. 10, Bandung 40132, Indonesia

^{*}E-mail: tmarhaendrajana@tm.itb.ac.id

Abstract. Wettability alteration during low salinity waterflooding (LSW) is expected to be one of the prominent reasons for enhanced oil recovery. However, the underlying mechanisms of improved oil recovery in sandstone during LSW are not entirely clear. Thus, a series of experiments was carried out to investigate the underlying mechanisms that drive the wettability alteration. FTIR spectroscopy was combined with thermogravimetric analysis to quantify the amount of adsorbed hydrocarbon components in sandstone with various clay contents. Afterward, the time-dependent contact angle in fabricated sandstone substrate (RMS roughness $9.91 \pm 1.31 \mu\text{m}$) was observed with various clay and brine contents to monitor the wettability alteration during LSW. The existence of divalent ions (Ca^{2+} and Mg^{2+}) was found to stabilize the sandstone and prevent it from swelling. Surprisingly, with the presence of divalent ions, the rate of contact angle change was insignificant ($\sim 1 - 4^\circ/\text{dilution}$), even though a reduction of divalent ions occurred and the rate of contact angle change with the sole presence of NaCl was notably altered ($\sim 6^\circ/\text{dilution}$). Furthermore, the presence of higher clay content showed an increased contact angle alteration. We propose that these phenomena are partially driven by macroscopic phenomena of clay swelling, which leads to surface roughening and enhances the water-wetness.

Keywords: *clay swelling; contact angle; enhanced oil recovery; low salinity waterflooding; surface roughness.*

1 Introduction

Many attempts to increase oil recovery have been done, such as chemical-based enhanced (surfactant [1-3], polymers [4,5], and alkaline solution [6-8]), heat-based (electromagnetic heating) oil recovery [9-21] and steam injection [12-14]), and microbial-based oil recovery to modify reservoir and crude oil properties [15,16]. However, environmental issues and high operational cost of the aforementioned enhanced oil recovery methods hamper their application in the field. Low salinity waterflooding is not a new method in the oil and gas industry. However, it is inexpensive, relatively environmentally friendly and straightforward operations are the main reasons it attracts interest from the

industry. Nevertheless, dissenting opinions on experimental facts among scientists have left the question about the mechanisms underlying the enhanced oil recovery during low salinity waterflooding unanswered as yet. Multiple mechanisms of low salinity waterflooding are expected to conspire to improve oil recovery. For sandstone reservoirs, several mechanisms have already been proposed, such as fines migration mechanism [17], ion exchange [18], and double layer expansion [19]. However, double layer expansion as the proposed mechanism has some limitations. It requires the presence of a water layer with a thickness of ~ 1 nm [20]. In addition, a unique characteristic of sandstone reservoirs should be noted, which is the presence of a high content of clay [21,22]. The clay has relatively high reactive behavior towards crude oil and water composition compared to the other components.

In sandstone reservoirs, reducing and altering the brine composition has led to promising additional recovery [17,23]. Further, several previous studies have studied low salinity waterflooding employing different techniques, from coreflooding [24], single-channel micromodel [25], contact angle measurement [26] to detailed nanoscale with atomic force microscopy [21]. Several researches have shown that there are essential requirements regarding enhanced oil recovery with low salinity waterflooding in sandstone. It has been observed that sandstone with clay minerals [21,22], crude oil with polar components [17], and formation water with divalent cations [18], such as Ca^{2+} and Mg^{2+} , are mandatory to drive the enhanced oil recovery in low salinity waterflooding. Divalent cations are well known as a bridge for crude oil polar components to the substrate, thus rendering the substrate more oil-wet [27,28].

As a result of multiple mechanisms of low salinity waterflooding, wettability alteration occurs and results in enhanced oil recovery. Many variables are linked to the wettability alteration, such as liquid surface tension, rock surface energy, surface roughness, crude oil properties, brine composition, etc. However, the contact angle value is a prominent parameter that incorporates all these variables. It has also been shown that by decreasing the divalent ion concentration, the wettability on the muscovite substrate is altered significantly, even though the ionic strength stays at a nearly constant level [29]. While reducing the ionic strength and only maintaining the divalent cation concentration, the contact angle did not change significantly [29].

The present study aimed to establish a novel understanding of how wettability alteration happens during low salinity waterflooding in sandstone reservoirs. Our series of experiments unambiguously showed a direct effect of brine composition and clay content on low salinity waterflooding in sandstone substrate (a mixture of quartz and clay granules).

2 Materials and Methods

Various types of characterizations were conducted to measure the amount of particular crude oil components that are adsorbed by the sandstone surface. First, an experiment was done to characterize the surface by thermogravimetric analysis (TGA). Subsequently, IR-spectroscopy was conducted to obtain information on the types of substances that are adsorbed into the sandstone surface. To that end, a fabricated sandstone surface was designed for measuring the time-dependent contact angle, which covers the essential rock components in the reservoir (presence of clay and surface roughness).

2.1 Crude Oil, Brine, and Injected Water Properties

In our experiments, heavy to moderate crude oil (API 35.59) was used. The crude oil contained 0.84% of asphaltenes and 4.82% of resins. The detailed properties of the crude oil sample are shown in Table 1.

Table 1 Crude oil properties used in this work.

Crude Oil Characteristic	Value
Saturated	61.22 %
Aromatics	33.12 %
Resins	4.82 %
Asphaltenes	0.84 %
EACN ^{b)} (Equivalent Alkane Carbon Number)	8.67
TAN (Total Acid Number)	1.207 mg KOH/g
Viscosity	0.90 cP (66 °C)
API Gravity	35.59

In the series of experiments, the brine and injected water used were prepared by mixing particular chemicals with demineralized water. All chemicals used were purchased from Sigma Aldrich. Variations were made in the ionic composition while maintaining the ionic strength of the brine below 10% deviation, as shown in Table 2.

Table 2 Brine composition for contact angle measurement used in this work.

Brine ID	NaCl (ppm)	CaCl ₂ (ppm)	MgCl ₂ (ppm)	Ionic Strength (mol/kg water)
A1	30000	-	-	1.144
B1	25000	2000	-	1.115
C1	25000	-	2000	1.184

2.2 Surface Fabrication and Characterization

The surface used for time-dependent contact angle measurement was fabricated by depositing a mixture of quartz (SiO_2) and clay granules on the glass. The quartz was provided by the Geological Department of ITB (maximum size 20 μm) and clay granules were purchased from PT UNIChem Candi Indonesia (size range from 2-4 μm). Initially, 10 gram of the clay and quartz granule mixture was conflated with 2 mL of demineralized water. The mixture was then stirred and polished onto the glass. Subsequently, the coated glass was heated at 100 °C for 1 hour. Then, the coated glass was aged by crude oil (by adding three drops of crude oil, ~0.15 mL) and heated again at 100 °C for 72 hours. Precisely 1 hour before usage, the coated glass was taken out of the oven and was cooled to room temperature and vacuumed for 1 hour. The surface was characterized by a profilometer (Mitutoyo Type SJ 301) with RMS roughness $9.91 \pm 1.31 \mu\text{m}$. Data from the X-ray diffraction analysis (RIGAKU SmartLab) of the clay granules are shown in Table 3.

Table 3 Mineralogy properties of clay granules used for surface fabrication.

Composition	Weight (%)
Quartz, SiO_2	5.8
Montmorillonite, $\text{Ca}_{0.2}(\text{Al}, \text{Mg})_2\text{Si}_4\text{O}_{10}(\text{OH})_2 \cdot 4\text{H}_2\text{O}$	48.2
Kaolinite, $\text{Al}_2\text{Si}_2\text{O}_5(\text{OH})_4$	20.7
Muscovite, $(\text{K}, \text{Na})\text{Al}_2(\text{Si}, \text{Al})_4\text{O}_{10}(\text{OH})_2$	25.3

2.3 Thermogravimetric Analysis

Thermogravimetric analysis (TGA) experiments were carried out to measure the adsorption of crude oil by the sandstone by Netzsch STA 449 F1 Jupiter. The sandstone samples were prepared by varying the content of clay and quartz granules based on weight. Five samples were used in this experiment with compositions as shown in Table 4.

Table 4 Clay granule compositions of the samples used.

Sample ID	Weight of Clay (%)
A2	0%
B2	10%
C2	20%
D2	30%
E2	40%

The mixture was aged with drops of crude oil (~0.15 mL crude oil/1 gr granule mixture) and left for 24 hours at 100 °C until the volatile components were evaporated. The TGA analysis was done using N₂ as a flowing gas phase, with a maximum temperature of 700 °C and a rate of 20 °C/min.

2.4 FTIR Spectroscopy

The C2 sandstone sample, crude oil, aged C2 sandstone sample were used for IR spectroscopy measurement. The aged C2 sandstone samples were prepared for IR spectroscopy through the same protocol as the sandstone sample for TGA. The IR spectra of the samples were recorded between 500 and 4000 cm⁻¹ on an IR spectrophotometer, ALPHA II FTIR Spectrometer. Subsequently, the sample was mixed with KBr as background.

2.5 Time-Dependent Contact Angle

Biolin Scientific ThetaLite 101 was employed for contact angle measurement. Subsequently, the data were measured by the Attension software. The detailed set-up is shown in Figure 1. Contact angle observation was conducted in captive drop orientation. The sandstone surface was immersed in 140 mL brine and crude oil droplets were injected at a volume of ~4 – 16 μL.

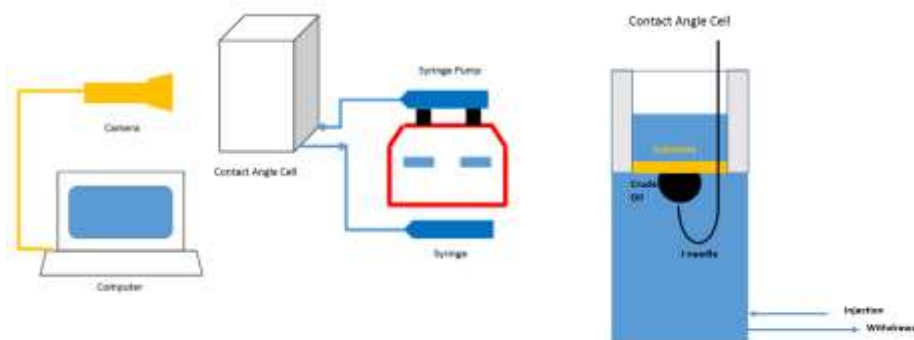


Figure 1 The experimental set-up used for contact angle measurement. The contact angle was measured in captive drop orientation.

The first 12 hours were used to stabilize the droplets on the surface. Next, sequential dilution was executed by reducing the salinity by half. The first series of experiments were conducted to observe the wettability alteration of the C2 surface with brine A1, B1, and C1. The second series of experiments were carried out to observe the wettability alteration of the B2, C2, and D2 surfaces with brine A1. Each experiment was conducted at least 3 times.

3 Results and Discussion

3.1 Thermogravimetric Analysis

The thermogravimetric results in Figure 2 show a significant mass loss difference between pure quartz and the mixture of quartz and clay granules of $\geq 6\%$. Interestingly, the difference between sandstone with varied clay content showed an insignificant difference ($\leq 2\%$). The results also showed that the higher the clay content, the more hydrocarbon component was adsorbed, which is expected to reduce the water-wetness of the substrate.

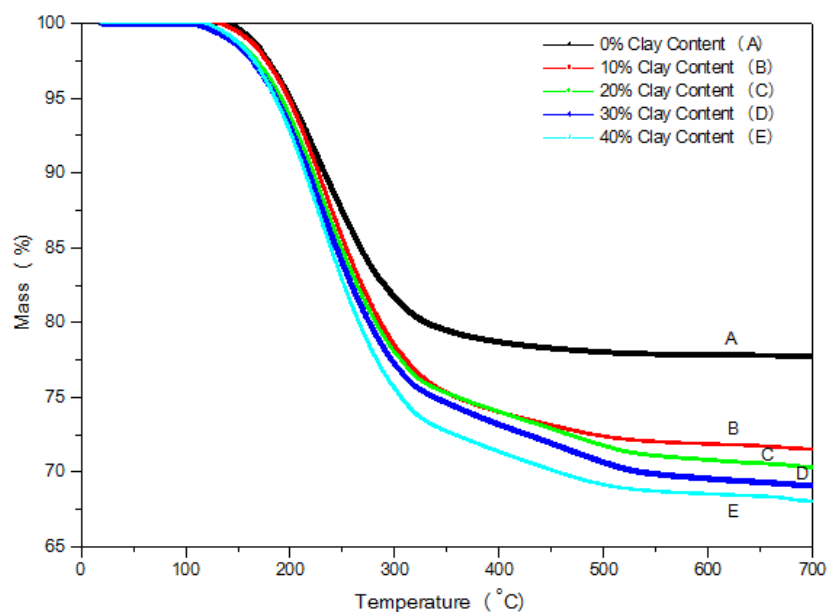


Figure 2 Thermogravimetric result.

3.2 FTIR Spectroscopy

The FTIR spectroscopy measurement used KBr as background. By comparing the IR spectroscopy results of the rock sample, the aged rock sample, and the crude oil sample it was shown that a particular component of the crude oil (wave number 2800-2940 cm^{-1}) was adsorbed into the aged rock sample, as shown in Figure 3. Clear adsorption of crude oil in the rock sample was indicated by the difference in IR spectroscopy results between the aged rock sample and the non-aged rock sample, as can be seen in Figure 4. Therefore, it was confirmed that the fabricated surface samples were adsorbed by hydrocarbon components from the crude oil sample.

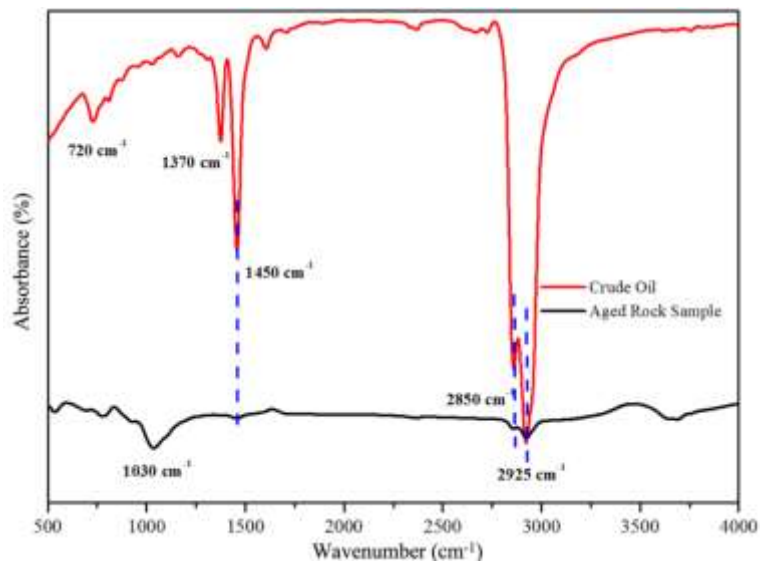


Figure 3 IR spectra for the crude oil and aged rock sample.

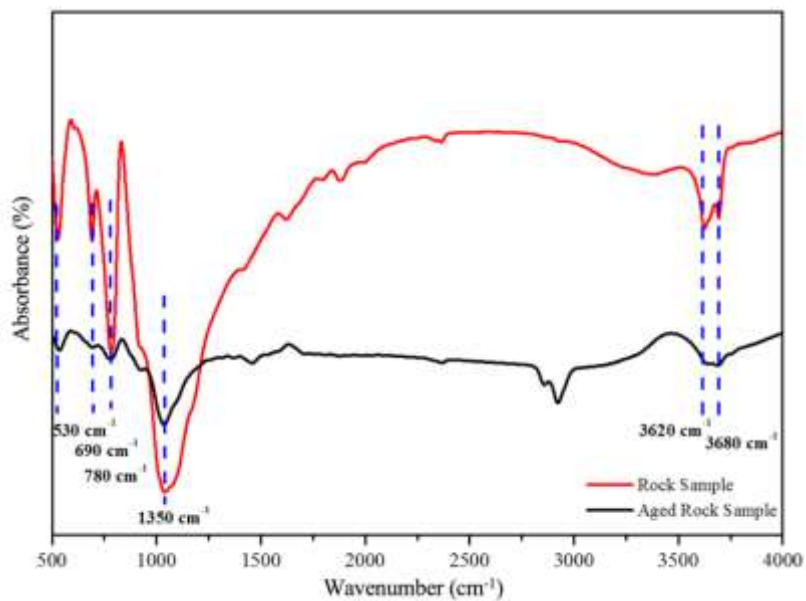


Figure 4 IR spectra of the rock sample and aged rock sample.

3.3 Time-Dependent Contact Angle

The dynamics of time-dependent contact angle in the stabilization phase (the initial 12 hours) are caused by the stabilization of macroscopic forces on the

droplets. Another factor governing the dynamics of the time-dependent contact angle during the stabilization phase is the presence of roughness. The space between the asperities is filled by a particular fraction of specific liquids. On the rough surface a wetting model can be employed, either the Wenzel or the Cassie-Baxter model [30]. Hence, the process to reach equilibrium force and fluid equilibrium fraction on a rough surface drives the contact angle alteration during the stabilization phase.

Figure 5 shows the time-dependent contact angle with brine variation for 20% clay fraction on the sandstone substrate. It shows that the presence of divalent ions (Ca^{2+} and Mg^{2+}) reduced the contact angle alteration compared to the sole presence of Na^+ . It was also observed that the inhibition of contact angle alteration by the presence of Mg^{2+} was lower compared to the presence of Ca^{2+} . Moreover, the presence of sulfate ions (SO_4^{2-}) in the brine did not alter the contact angle value. During the initial stabilization phase, with 30000 ppm NaCl eq, the surface containing 20% clay showed approximately the same value for water contact angle ($\sim 45^\circ$) with different brine compositions. In addition, direct observation showed severe clay swelling in the brine A1 sample as salinity decreased, while the presence of divalent cations stabilized the clay.

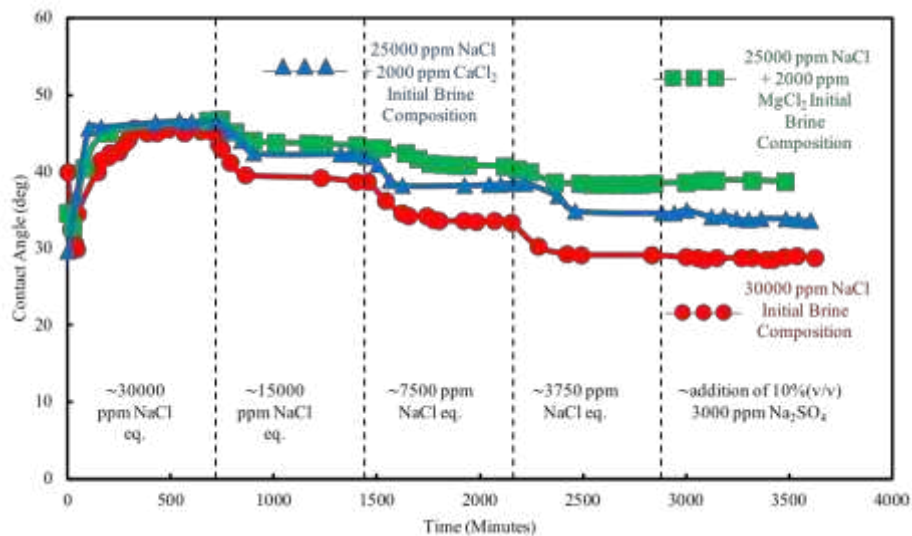


Figure 5 Time-dependent contact angle for sandstone with 20% clay content at different brine compositions.

The time-dependent contact angle with clay variation on the surface depicted in Figure 6 shows that the more clay is present, the higher the initial water contact angle. In the subsequent dilutions, it was shown that the water contact angle of

the three surface samples (10%, 20%, and 30% clay) had approximately the same water contact angle ($\sim 33^\circ$). It was shown that the higher the clay content, the higher the contact angle alteration.

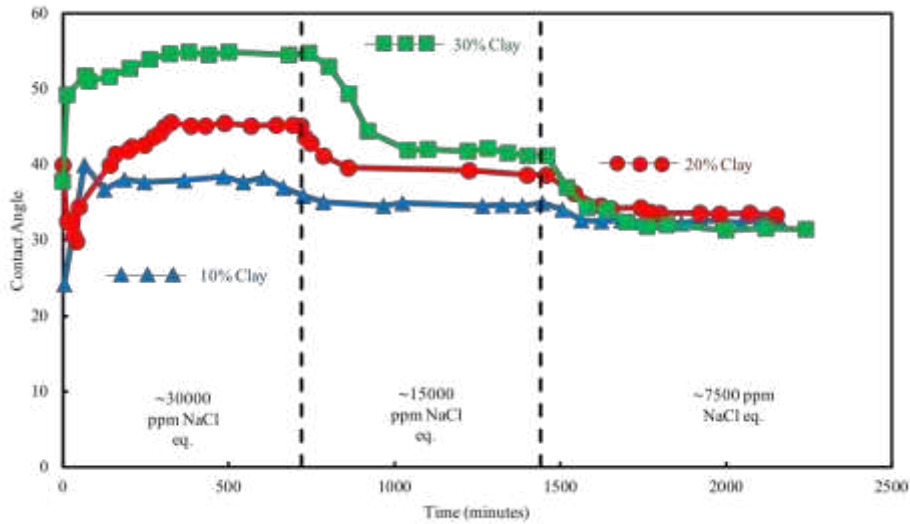


Figure 6 Time-dependent contact angle in sandstone with various clay contents for 30000 ppm NaCl initial brine composition.

By considering the DLVO theory, the repulsion and attraction force at the interface of the substrate and the crude oil are the main factors to explain the wettability alteration phenomena. There are three major contributing forces in the interface, which are a double layer, the Van der Waals force, and the hydration force, as shown in Eq. (1). In oil and rock interfaces, the Van der Waals force is attractive while the electrostatic force is repulsive. The solvation force, a non-DLVO force, can be either repulsive or attractive depending on the specific surface, solvent, and solute properties. The solvation force influences the system at a lower separation distance of the two surfaces and therefore needs to be measured at high salinity condition. However, the hydration force and the Van der Waals force vary insignificantly in various salinity conditions [21,29]. Furthermore, a mechanism was examined that may be responsible for the observed wettability alteration, called the double layer effect. The double layer thickness in this system was calculated using Eq. (2) [31]:

$$F(d)_{total} = F(d)_{vdW} + F(d)_{el} + F(d)_{sol} \tag{1}$$

$$\kappa^{-1} = \sqrt{\left(\frac{\epsilon\epsilon_0 kT}{2N_A e^2 I}\right)} \tag{2}$$

where ε is the relative electric permittivity, ε_0 is the electric permittivity, k is the Boltzmann constant, T is the bulk temperature, and κ^{-1} is the Debye length. Figure 7 shows that it is not possible with all experimental conditions to have a bulk water layer. Our calculations showed that the maximum Debye length (Eq. (1)) after the 3rd dilution was 0.81 nm. Therefore, without the presence of a bulk water layer, double layer contraction does not occur. Although an ion-exchange mechanism is present [18,19], it cannot be the sole factor responsible for the wettability alteration since the contact angle does not alter significantly with the presence of divalent cations.

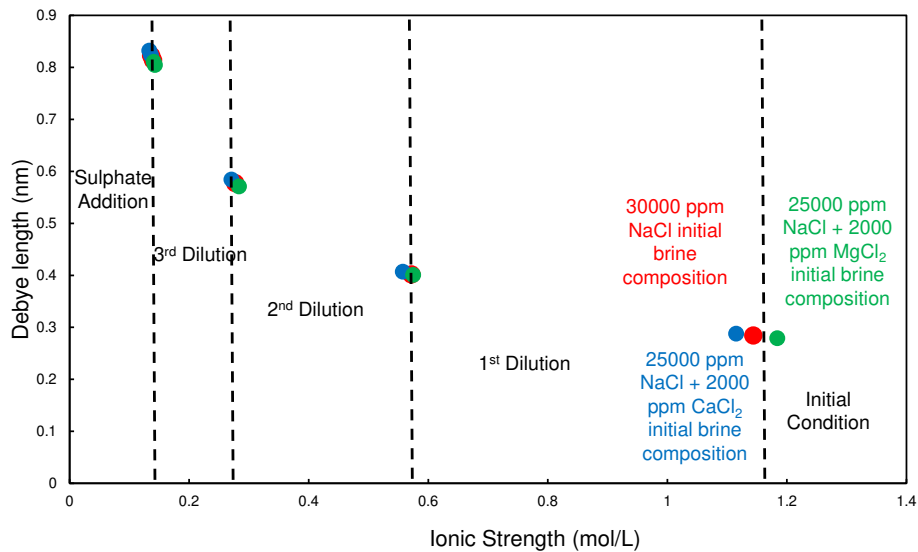


Figure 7 Debye length calculation against ionic strength.

In response to incompatible existing mechanisms to explain our experimental result, we observe that clay swelling likely drives another mechanism during low salinity waterflooding. Clay swelling may increase the volume of the clay up to 10 times of the normal volume. Furthermore, severe swelling generates increased surface roughness. The presence of higher surface roughness enhances the water-wetness of the surface as shown in Figures 8 and 9. The presence of divalent cations minimizes the clay swelling effect. Furthermore, severe swelling occurs with the presence of NaCl only. The wetting phenomena on a rough surface interpreted by the apparent contact angle should be described. A simple equation that can explain this phenomenon is described by the Wenzel model (Eq. (3)) and the Cassie-Baxter model (Eq. (4)) [30]. Apparently, the Wenzel and Cassie-Baxter models are corollaries of the physical influence of the increase of surface roughness. However, the Wenzel

and Cassie-Baxter models measure the meta-stable thermodynamic equilibrium in the presence of surface roughness.

$$\cos \theta_a = r \cos \theta \tag{3}$$

$$\cos \theta_a = 1 - f + rf \cos \theta \tag{4}$$



Figure 8 Illustration of surface roughening effect after low salinity waterflooding. The enhanced surface roughness leads to a more water-wet system.

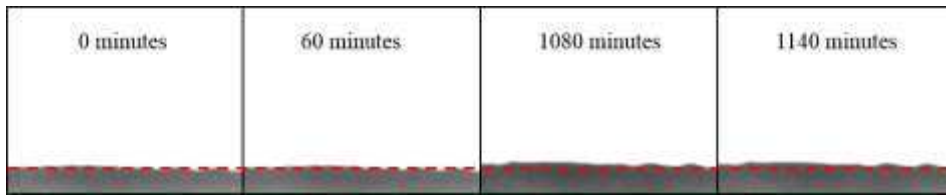


Figure 9 The visualization of surface roughening during low salinity injection in 10% clay substrate. At time = 0 minutes, the salinity was 30000 ppm NaCl, and was sequentially diluted until time = 1140 minutes with 7500 ppm NaCl. Each picture represents 0.5 mm x 0.64 mm; the red dotted line is for guiding the eye.

Where θ_a is the apparent water contact angle, θ is the intrinsic water contact angle, r is the surface roughness, f is the area fraction of surface wetted by water. The Wenzel model shows that the presence of surface roughness always higher than 1 ($r \geq 1$) leads to enhanced water-wetness if the intrinsic contact angle is $\leq 90^\circ$. The Cassie-Baxter model shows a different system. Since $0 \leq f \leq 1$, for instance, a system on a very rough surface, $r \geq 3$, with intrinsic contact angle $\leq \sim 70^\circ$ and a higher fraction of surface wetted by water $f \geq \sim 0.7$, would enhance the water-wetness. In other words, the increase of surface roughening enhances the wettability of the wetting liquid. In this case, the presence of surface roughening enhances the wettability alteration of rock makes it more water-wet. Regardless of roughness and area fraction wetted by

water, the theories of Wenzel and Cassie-Baxter do not depend on the geometry or arrangement of the roughness [32]. This is important because the surface roughness of the substrate is irregular.

Further, we should note that the two models are very different in terms of adhesion because the Wenzel model is highly attached compared to the Cassie-Baxter model. We expect that the Cassie-Baxter state plays an important role during wettability alteration and drives the enhanced oil recovery during low salinity waterflooding. Nevertheless, more investigation is needed to examine the threshold for clay swelling that does not lead to pore blocking.

4 Conclusions

Various mechanisms for enhanced oil recovery by low salinity waterflooding in sandstone reservoirs have been proposed. Wettability alteration is often seen as a cause rather than a consequence. Although this is disputable, in this study, the wettability alteration was considered as a consequence and an attempt was made to unravel the factors that drive the wettability alteration.

In this work, the alteration of the contact angle during low salinity water flooding was studied using a modified contact angle cell that incorporates deionized water pumping. The experiment used a quartz and clay mixture aged with droplets of oil. Both samples were characterized beforehand using various methods, i.e. FTIR, TGA, and profilometer.

In the present report, the FTIR and TGA results showed that a substrate with higher clay content tends to adsorb a higher fraction of crude oil. This indicates that the substrate system will be more oil-wet in the presence of clay. Further, our finding on the time-dependent contact angle showed that one of the major macro-mechanisms that drives wettability alteration is surface roughening by clay swelling. Based on the Cassie-Baxter state, a roughened surface drives the wetting towards water-wetness. In addition, the presence of divalent ions stabilizes the clay and inhibits the surface roughening process. Hence, the threshold for clay swelling needs to be determined for eliminating the pore blocking effect.

Wettability alteration due to surface roughening may cause the adsorbed oil not to be released from the rock surface. Instead, it may change the relative permeability, hence reducing the water/oil mobility ratio, which results in much better oil sweeping by water, thus increasing overall oil recovery. However, the oil recovery consequences are not covered in this article, it solely focuses on how surface roughening alters the oil/rock/water system. To that end, the further study regarding this effect on oil recovery needs to be investigated.

5 Acknowledgements

This work was supported and funded by Lembaga Penelitian dan Pengabdian Masyarakat Institut Teknologi Bandung (LPPM ITB). The authors thank Prof. Thomas A. Blasingame for our fruitful discussions. The authors also acknowledge the assistance of Mr. Abdel MD for the contact angle measurement.

References

- [1] Adams, W.T. & Schievelbein, V.H., *Surfactant Flooding Carbonate Reservoirs*, SPE Reservoir Engineering, **2**(04), pp. 619-626, 1987.
- [2] Lohne, A. & Fjelde, I., *Surfactant Flooding in Heterogeneous Formations*, in SPE Improved Oil Recovery Symposium, Society of Petroleum Engineers: Tulsa, Oklahoma, USA, 2012.
- [3] Hakiki, F., Maharsi, D.A. & Marhaendrajana, T., *Surfactant-Polymer Coreflood Simulation and Uncertainty Analysis Derived from Laboratory Study*, Journal of Engineering and Technological Sciences, **47**(6), pp. 706-724, 2015.
- [4] Seright, R.S., Seheult, J.M. & Talashek, T., *Injectivity Characteristics of EOR Polymers*, in SPE Annual Technical Conference and Exhibition Society of Petroleum Engineers, Denver, Colorado, USA, 2008.
- [5] Needham, R.B. & Doe, P.H., *Polymer Flooding Review*, Journal of Petroleum Technology, **39**(12), pp. 1503-1507, 1987.
- [6] Evans, D.B., Stepp, A.K. & French, T., *Improved Crude Oil Recovery by Alkaline Flooding Enhanced with Microbial*, in SPE/DOE Improved Oil Recovery Symposium, Society of Petroleum Engineers: Tulsa, Oklahoma, USA, 1998.
- [7] Falls, A.H., Thigpen, D.R., Nelson, R.C. & Shahin, G.T., *Field Test of Cosurfactant-Enhanced Alkaline Flooding*, SPE Reservoir Engineering, **9**(3), p. 217-223, 1994.
- [8] Surkalo, H., *Enhanced Alkaline Flooding*, Journal of Petroleum Technology, **42**(01), pp. 6-7, 1990.
- [9] Chakma, A. & Jha, K.N., *Heavy-Oil Recovery From Thin Pay Zones by Electromagnetic Heating*, in SPE Annual Technical Conference and Exhibition, Society of Petroleum Engineers: Washington, D.C., USA, 1992.
- [10] Sahni, A., Kumar, M. & Knapp, R.B., *Electromagnetic Heating Methods for Heavy Oil Reservoirs*, in SPE/AAPG Western Regional Meeting, Society of Petroleum Engineers: Long Beach, California, USA, 2000.
- [11] Carrizales, M.A., Lake, L.W. & Johns, R.T., *Production Improvement of Heavy-Oil Recovery by Using Electromagnetic Heating*, in SPE Annual

- Technical Conference and Exhibition, Society of Petroleum Engineers: Denver, Colorado, USA, 2008.
- [12] Wu, S., He, L., Wenlong, G., Dehuang, S., Yu, Q. & Lihua, L., *Steam Injection in A Waterflooding, Light Oil Reservoir*, in International Petroleum Technology Conference, International Petroleum Technology Conference: Kuala Lumpur, Malaysia, 2008.
- [13] Memarzadeh, A. & Rahnema, H., *Thermodynamic Analysis of Solvent Assisted Steam Injection*, in SPE Annual Technical Conference and Exhibition, Society of Petroleum Engineers: Houston, Texas, USA, 2015.
- [14] Morlot, C. & Mamora, D.D., *TINBOP Cyclic Steam Injection Enhances Oil Recovery in Mature Steamfloods*, in Canadian International Petroleum Conference, Petroleum Society of Canada: Calgary, Alberta, 2007.
- [15] Ghadimi, M.R. & Ardjmand, M., *Simulation of Microbial Enhanced Oil Recovery*, in International Oil Conference and Exhibition in Mexico, Society of Petroleum Engineers, Cancun, Mexico, 2006.
- [16] Bae, J.H., Chambers, K.T. & Lee, H.O., *Microbial Profile Modification with Spores*, SPE Reservoir Engineering, **11**(03): pp. 163-167, 1996.
- [17] Tang, G-Q. & Morrow, N.R., *Influence of Brine Composition and Fines Migration on Crude Oil/Brine/Rock Interactions and Oil Recovery*, Journal of Petroleum Science and Engineering, **24**(2), pp. 99-111, 1999.
- [18] Lager, A., Webb, K.J., Black, C.J.J., Singleton, M. & Sorbie, K.S., *Low Salinity Oil Recovery- An Experimental Investigation*, International Symposium of the Society of Core Analysts, 2006.
- [19] Myint, P.C. & Firoozabadi, A., *Thin Liquid Films in Improved Oil Recovery from Low-Salinity Brine*, Current Opinion in Colloid & Interface Science, **20**(2), pp. 105-114, 2015
- [20] Yutkin, M.P., Mishra, H., Patzek, T.W., Lee, J. & Radke, C.J., *Bulk and Surface Aqueous Speciation of Calcite: Implications for Low-Salinity Waterflooding of Carbonate Reservoirs*, SPE Journal, **23**(1), pp. 84-101, 2018
- [21] Mugele, F., Bera, B., Cavalli, A., Siretanu, I., Maestro, A., Duits, M., Cohen-Stuart, M., Ende, D.v.d., Stocker, I. & Collins, I., *Ion Adsorption-induced Wetting Transition in Oil-water-mineral Systems*, Scientific Reports, **5**, p. 10519, 2015.
- [22] Mohan, K., Gupta, R. & Mohanty, K.K., *Wettability Altering Secondary Oil Recovery in Carbonate Rocks*. Energy & Fuels, **25**(9), pp. 3966-3973, 2011.
- [23] Jadhunandan, P.P. & Morrow, N.R., *Effect of Wettability on Waterflood Recovery for Crude-Oil/Brine/Rock Systems*, SPE Reservoir Engineering, **10**(1), pp. 40-46, 1995.
- [24] Ishiwata, T., Kurihara, M., Taniguchi, H., Tsuchiya, Y., Watanabe, J. & Matsumoto, K., *Investigation on Low Salinity Waterflooding Through Core Flooding Experiments and Numerical Simulation*, in 22nd Formation

- Evaluation Symposium of Japan, Society of Petrophysicists and Well-Log Analysts: Chiba, Japan, 2016
- [25] Bartels, W.B., Mahani, H., Berg, S., Menezes, R., van der Hoeven, J.A. & Fadili, A., *Oil Configuration Under High-Salinity and Low-Salinity Conditions at Pore Scale: A Parametric Investigation by Use of a Single-Channel Micromodel*, SPE Journal, **22**(5), pp. 1362-1373, 2017.
 - [26] Mahani, H., Berg, S., Illic, D., Bartels, W.B. & Joekar-Niasar, V., *Kinetics of Low-Salinity-Flooding Effect*, SPE Journal, **20**(1), pp. 8-20, 2015.
 - [27] Mugele, F., Siretanu, I., Kumar, N., Bera, B., Wang, L., Ruitter, R.d., Maestro, A., Duits, M., Ende, D.v.d. & Collins, I., *Insights From Ion Adsorption and Contact-Angle Alteration at Mineral Surfaces for Low-Salinity Waterflooding*, SPE Journal, **21**(4), pp. 1204-1213, 2016.
 - [28] Qi, Z., Wang, Y., He, H., Li, D. & Xu, X., *Wettability Alteration of the Quartz Surface in the Presence of Metal Cations*, Energy & Fuels, **27**(12), pp. 7354-7359, 2013.
 - [29] Haagh, M.E.J., Siretanu, I., Duits, M.H.G. & Mugele, F., *Salinity-Dependent Contact Angle Alteration in Oil/Brine/Silicate Systems: the Critical Role of Divalent Cations*, Langmuir, **33**(14), pp. 3349-3357, 2017.
 - [30] Whyman, G., E. Bormashenko, & Stein, T., *The Rigorous Derivation of Young, Cassie–Baxter and Wenzel Equations and the Analysis of the Contact Angle Hysteresis Phenomenon*, Chemical Physics Letters, **450**(4-6), pp. 355-359, 2008.
 - [31] Mahani, H., Menezes, R., Berg, S., Fadili, A., Nasralla, R., Voskov, D. & Joekar-Niasar, V., *Insights into the Impact of Temperature on the Wettability Alteration by Low Salinity in Carbonate Rocks*, Energy & Fuels, **31**(8), pp. 7839-7853, 2017.
 - [32] Calvimontes, A., *Thermodynamic Equilibrium in the Wetting of Rough Surfaces*, Raleigh, NC: Lulu Press, Inc, 2014.